Stem Cell Reports

Article

Pluripotent Stem Cell Model of Nakajo-Nishimura Syndrome Untangles Proinflammatory Pathways Mediated by Oxidative Stress

Fumiko Honda-Ozaki,[1,7] Madoka Terashima,[1,7] Akira Niwa,[1] Norikazu Saiki,[1] Yuri Kawasaki,[1] Haruna Ito,[1] Akitsu Hotta,[2] Ayako Nagahashi,[3] Koichi Igura,[3] Isao Asaka,[3] Hongmei Lisa Li,[2,4] Masakatsu Yanagimachi,[5] Fukumi Furukawa,[6] Nobuo Kanazawa,[6,8,*] Tatsutoshi Nakahata,[1] and Megumu K. Saito[1,8,*]

[1]Department of Clinical Application, Center for iPS Cell Research and Application, Kyoto University, Kyoto 606-8507, Japan
[2]Department of Life Science Frontiers, Center for iPS Cell Research and Application, Kyoto University, Kyoto 606-8507, Japan
[3]Department of Fundamental Cell Technology, Center for iPS Cell Research and Application, Kyoto University, Kyoto 606-8507, Japan
[4]Boston Children's Hospital, Harvard Medical School, Boston, MA 02115, USA
[5]Department of Pediatrics, Tokyo Medical and Dental University, Tokyo 113-8519, Japan
[6]Department of Dermatology, Wakayama Medical University, Wakayama 641-0012, Japan
[7]Co-first author
[8]Co-senior author
*Correspondence: nkanazaw@wakayama-med.ac.jp (N.K.), msaito@cira.kyoto-u.ac.jp (M.K.S.)
https://doi.org/10.1016/j.stemcr.2018.04.004

SUMMARY

Nakajo-Nishimura syndrome (NNS) is an immunoproteasome-associated autoinflammatory disorder caused by a mutation of the *PSMB8* gene. Although dysfunction of the immunoproteasome causes various cellular stresses attributed to the overproduction of inflammatory cytokines and chemokines in NNS, the underlying mechanisms of the autoinflammation are still largely unknown. To investigate and understand the mechanisms and signal pathways in NNS, we established a panel of isogenic pluripotent stem cell (PSC) lines with *PSMB8* mutation. Activity of the immunoproteasome in *PSMB8*-mutant PSC-derived myeloid cell lines (MT-MLs) was reduced even without stimulation compared with non-mutant-MLs. In addition, MT-MLs showed an overproduction of inflammatory cytokines and chemokines, with elevated reactive oxygen species (ROS) and phosphorylated p38 MAPK levels. Treatment with p38 MAPK inhibitor and antioxidants decreased the abnormal production of cytokines and chemokines. The current PSC model revealed a specific ROS-mediated inflammatory pathway, providing a platform for the discovery of alternative therapeutic options for NNS and related immunoproteasome disorders.

INTRODUCTION

Autoinflammatory disorders caused by the dysfunction of proteasomes have been collectively designated as proteasome-associated autoinflammatory syndromes (PRAASs) (Almeida de Jesus and Goldbach-Mansky, 2013; Brehm et al., 2015; McDermott et al., 2015). PRAASs were originally defined as mutations in the immunoproteasome component of *proteasome subunit beta 8* (*PSMB8*) gene, but have been since expanded to include the dysregulation of both the constitutive proteasome and the immunoproteasome (Brehm et al., 2015; McDermott et al., 2015). PRAASs include Nakajo-Nishimura syndrome (NNS; also known as autoinflammation, lipodystrophy, and dermatosis syndrome) (Arima et al., 2011), Japanese autoinflammatory syndrome with lipodystrophy (Kitamura et al., 2011), joint contractures, muscular atrophy, microcytic anemia, panniculitis-associated lipodystrophy syndrome (Garg et al., 2010), and chronic atypical neutrophilic dermatosis with lipodystrophy and elevated temperature (CANDLE) syndrome (Brehm et al., 2016; Liu et al., 2012). NNS is an autosomal recessive disorder caused by a homozygous mutation in the *PSMB8* gene (Arima et al., 2011; Kitamura et al., 2011). Patients with NNS show pernio-like skin rashes from infancy and grad-

ually develop partial lipodystrophy mainly in the face and upper extremities, as well as show characteristically long clubbed fingers with contracture of the interphalangeal joints. Patients also suffer from remittent fever and nodular erythema-like skin eruptions (Arima et al., 2011; Kunimoto et al., 2013). Although the administration of systemic corticosteroids is partially effective, particularly against skin lesions, the prognosis remains relatively poor since this therapy is ineffective on lipodystrophy. Since there is currently no curative therapy for NNS and most patients die as a result of respiratory or cardiac failure (Arima et al., 2011; Kanazawa, 2012), therapeutic advances for NNS are desired.

Proteasomes are highly efficient proteolytic machinery for degrading damaged or unnecessary proteins (van Deventer and Neefjes, 2010). *PSMB8* gene encodes β5i protein, which is a subunit of a specialized type of proteasome named immunoproteasome. The catalytic component of the constitutive proteasome consists of three protease subunits: chymotrypsin-like enzyme β5, trypsin-like enzyme β2, and caspase-like enzyme β1 (Murata et al., 2009; Reis et al., 2011). These three subunits correspond to immunoproteasome subunits β5i, β2i, and β1i, respectively. The immunoproteasome is constitutively expressed in hematopoietic cells (McCarthy and Weinberg, 2015; Roccaro

et al., 2010). In addition, in immune cells, immunoproteasome subunits are upregulated and replace their corresponding constitutive proteasome subunits upon stimulation with proinflammatory cytokines such as interferon gamma (IFN-γ) and tumor necrosis factor alpha (TNF-α) (Kimura et al., 2015; McCarthy and Weinberg, 2015). The immunoproteasome has a role in processing endogenous peptides that are presented on major histocompatibility complex I molecules (Groettrup et al., 2010; Reis et al., 2011).

Almost all Japanese NNS patients share the same homozygous point mutation, c.602G > T, which causes substitution of glycine 201 to valine (Arima et al., 2011; Kunimoto et al., 2013). NNS-associated *PSMB8* mutations cause impaired assembly of the immunoproteasome, resulting in a reduction of immunoproteasome activity in immune cells. This impaired immunoproteasome activity causes an accumulation of ubiquitinated and oxidized proteins (Arima et al., 2011) and is attributed to the elevation of the serum concentration of several proinflammatory cytokines and chemokines, such as IL-6, IP-10 and MCP-1 in NNS patients (Arima et al., 2011). Although involvement of the p38 mitogen-activated protein kinase (p38 MAPK) pathway in the upregulation of proinflammatory cytokines was implicated in NNS patients (Arima et al., 2011), the precise pathway harnessing immunoproteasome dysfunction to the overproduction of proinflammatory cytokines remains unclear.
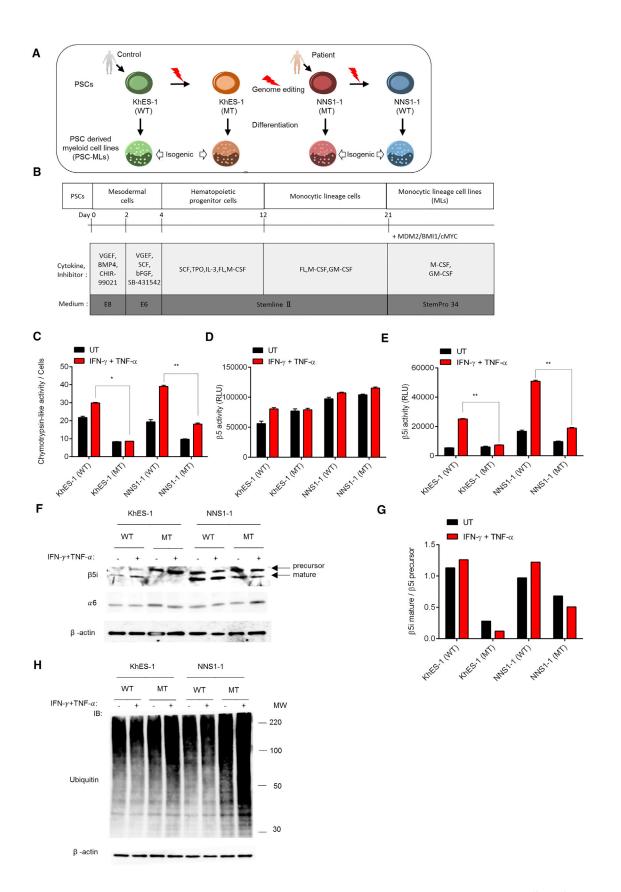
Among PRAASs, CANDLE syndrome has recently been recognized as an IFN-driven disease and shows a prominent IFN signature (Liu et al., 2012). A JAK inhibitor, baricitinib, is currently undergoing clinical trial (clinicaltrials.gov: NCT01724580) (Jabbari et al., 2015). On the other hand, although NNS and CANDLE share the same responsible gene, whether NNS symptoms are also driven by the IFN pathway has not been clarified. To investigate the detailed mechanism and signal pathways in NNS as well as to seek potential therapeutic candidates, in the current study we focused on establishing a pluripotent stem cell (PSC) model using NNS patient-derived induced pluripotent stem cells (iPSCs) and isogenic controls. We then recapitulated the *in vitro* phenotypes of NNS by differentiating the iPSCs into myeloid cell lines (PSC-MLs) (Haruta et al., 2013). NNS-PSC-MLs showed reduced proteasome activity and increased production of IL-6, MCP-1, and IP-10. Since these phenotypes corresponded to those of patient-derived peripheral blood monocytes, we concluded that our *in vitro* NNS-iPSC model successfully recapitulated the patient condition. We then validated several compounds for ameliorating the proinflammatory responses of NNS. Our isogenic PSC models are useful for elucidating the pathophysi-

ology of NNS and also for providing a platform for high-throughput drug screening.

RESULTS

Establishment of NNS-iPSCs and the Generation of Isogenic PSC Panels

Dermal fibroblasts were obtained from three NNS patients who shared the same homozygous mutation of *PSMB8* gene (Table S1, p.G201V [c.602G > T]) (Arima et al., 2011). The clinical features of all three NNS cases are summarized in Table S1. These fibroblasts were reprogrammed by introducing retroviral vectors encoding OCT3/4, SOX2, KLF4, and cMYC (Takahashi et al., 2007). Two iPSC clones from each NNS patient were randomly selected and propagated. All iPSC clones showed a typical characteristic human embryonic stem cell (ESC)-like morphology (Figure S1A) and expressed PSC-specific markers NANOG and SSEA4 (Figure S1A). The expression of residual transgenes was rarely detected (Figure S1B). All iPSC clones also maintained a normal karyotype (Figure S1C), and their pluripotency was confirmed by the formation of teratomas composed of all three germ layers (Figure S1D). The chymotrypsin-like activity of undifferentiated patient-derived iPSCs was comparable to that of the control PSCs even after IFN-γ and TNF-α stimulation (Figure S1E). Since all 6 NNS-iPSC clones from three individuals exhibited similar characteristics, including hematopoietic differentiation efficiency (Table S2), we selected a representative iPSC clone from patient 1 (NNS1-1, hereafter referred to as NNS1-1 [MT]) and used it for the subsequent analysis. To precisely evaluate the mutant-specific phenotype, we attempted to generate isogenic iPSCs by correcting the corresponding *PSMB8* mutation using the CRISPR-Cas9 (D10A) nickase-mediated double-nicking system (Ran et al., 2013; Zhou et al., 2014) (Figures 1A and S2A). We tested two single-guide RNA (sgRNA) sequences for each breakpoint and found that the sgRNA pair sg1-2/sg2-1 showed the highest rate of homozygous recombination-mediated gene replacement: out of three puromycin-resistant clones analyzed, one clone was heterozygously targeted and two clones were homozygously targeted (Figure S2B). Hereafter, we selected the homozygously targeted clone, referred to as NNS1-1 (WT), which was validated by a genomic PCR (Figure S2C). The loxP-flanked puromycin selection cassette was removed from each targeted iPSC clone by transient transfection with a vector expressing Cre recombinase. We also checked the T-to-G homozygous correction on exon 5 of the *PSMB8* gene by Sanger sequencing (Figure S2D). In a similar way, we generated homozygous *PSMB8*-G201V

(legend on next page)

knockin PSCs from a control human ESC line, KhES-1 (referred to as KhES-1 [WT] for control KhES-1, and KhES-1 [MT] for *PSMB8*-mutated KhES-1; Figures 1A and S2E–S2G). It was previously shown that the selective inhibition of two immunoproteasome subunits (β1i and β5i) results in the downregulation of several pluripotency markers in human ESCs (Atkinson et al., 2012), indicating immunoproteasome subunits may affect the maintenance of pluripotency. However, in our hands, there was no difference in the expression of PSC-associated markers and *in vivo* pluripotency between MT- and WT-clones (Figures S1A, S1B, and S1D). The efficiency of reprogramming and the efficiency of genome editing were also comparable between MT- and WT-clones (Table S2 and Figures S2C and S2F). Therefore, at least in this study, the disease-associated mutant *PSMB8* seemed not to affect the biological features of undifferentiated PSCs. Overall, we successfully established isogenic disease-control pairs using patient-derived iPSCs and genome-editing technology, which enabled us to precisely evaluate the effects of the disease-causing *PSMB8* mutation in PSC-derived differentiated cells.

Impairment of Immunoproteasome Activity in *PSMB8*-Mutant PSC-Derived Monocytic Cell Lines

Previous histopathological examination of the inflammatory sites in NNS patients has shown the infiltration of CD68^{+}, myeloperoxidase-positive monocytic cells and CD3^{+} T cells (Kunimoto et al., 2013). Since macrophages are the primary source of inflammatory cytokines and predominantly express the immunoproteasome (Ebstein et al., 2012; McCarthy and Weinberg, 2015), we focused on the *in vitro* phenotypes of differentiated monocytic cells from PSCs. CD14^{+} monocytes were differentiated from PSCs according to a previously described protocol with approximately 90% purity (Figures 1B and S3A) (Yanagimachi et al., 2013). To stably obtain an unlimited number of differentiated cells, PSC-derived monocytes were immortalized by transducing lentivirus vectors that encoded MDM2, BMI1, and cMYC (Haruta et al., 2013; Kawasaki et al., 2017) (Figure 1B). The established

PSC-derived monocytic cell lines (PSC-MLs) maintained the expression of monocyte markers CD14 and CD33 (Figure S3A) and showed a morphology that was compatible with monocytic cells (Figure S3B). We measured the proteasome activity, especially the chymotrypsin-like activity in PSC-MLs, using a luciferase-based proteasome assay. When the immunoproteasome assembly was induced by IFN-γ and TNF-α, we observed an upregulation of chymotrypsin-like activity in wild-type PSC-MLs (WT-MLs) (Figure 1C). However, this upregulation was not observed in mutant PSC-MLs (MT-MLs) (Figure 1C). When the activity levels of β5 and β5i were separately evaluated in the IFN-γ- and TNF-α-treated PSC-MLs, we found the activity of constitutive subunit β5 was not affected in any PSC-ML (Figure 1D). In contrast, although treatment of WT-MLs with IFN-γ and TNF-α elevated the immunoproteasome subunit β5i activity, the activity was significantly lower in NNS1-1-(MT)-MLs, and there was no elevation in β5i activity in KhES-1-(MT)-MLs (Figure 1E). Notably, the baseline activity of β5i was already decreased in both MT-MLs (Figure 1E), possibly due to the constitutive expression of immunoproteasome proteins in hematopoietic cells (McCarthy and Weinberg, 2015). The decreased chymotrypsin-like activity in IFN-γ- and TNF-α-treated cells was confirmed in primary monocytes from NNS patients (Figure S3C). Since all proteasome β subunits except β3 and β4 are translated as precursors containing N-terminal pro-regions (Yun et al., 2016), we next evaluated the maturation of β5i protein in PSC-MLs. When untreated, β5i was constitutively expressed in both WT-MLs and MT-MLs, but its maturation was relatively impaired in MT-MLs (Figures 1F and 1G). Other proteasome subunits were also expressed in PSC-MLs (Figure S3D). When treated with IFN-γ and TNF-α, the maturation of β2i and β1i was also impaired in MT-MLs (Figure S3D). MT-MLs showed an accumulation of ubiquitinated proteins in comparison with WT-MLs not only with IFN-γ and TNF-α stimulation, but also in an untreated state (Figure 1H). These data support the physiological dysfunction of the immunoproteasome machinery in *PSMB8*-mutant PSC-derived monocytic cells.

Figure 1. The Establishment of an Isogenic PSC Panel for NNS Study
(A) Study design.
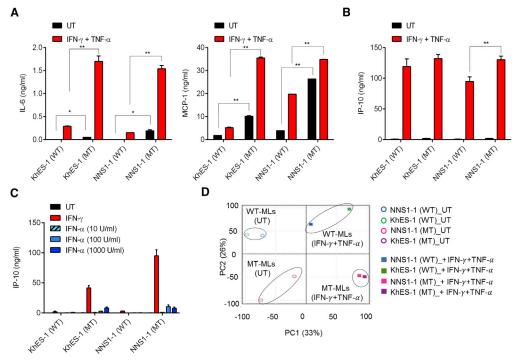(B) The protocol for monocytic differentiation and the establishment of PSC-MLs.
(C–E) The chymotrypsin-like activity of PSC-MLs was measured by a luciferase-based assay. The chymotrypsin-like activity was normalized according to the number of cells. The chymotrypsin-like proteolytic activities of constitutive proteasome (D, β5 subunit) and immunoproteasome (E, β5i subunit) in PSC-MLs. Background fluorescence or luminescence was subtracted from each value. Bars indicate the means ±SD (n = 3). Asterisks indicate statistically significant differences by Student's t test: *p < 0.05; **p < 0.01.
(F) Western blotting of immunoproteasome subunits β5i and α6.
(G) The quantity of mature β5i in (F) was normalized by the expression of immature β5i.
(H) Western blotting of ubiquitinated proteins.
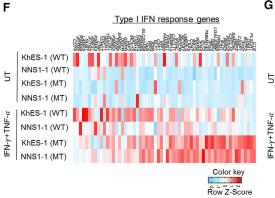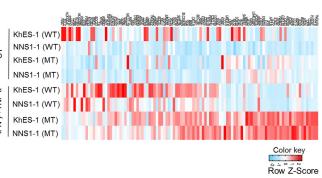In (C)–(H), the cells were treated with IFN-γ (100 ng/mL) and TNF-α (100 ng/mL) for 20 hr.

A

B

C

D

E

Enrichment in MT-ML lines > WT-ML line (IFN-γ+TNF-α)

Pathway	Source	Gene set size	Enrichment score (ES)	Normalized ES	NOM p-value	FDR q-value
INTERFERON_GAMMA_RESPONSE	Hallmarks	110	0.57748294	2.161759	0	0
INFLAMMATORY_RESPONSE	Hallmarks	119	0.557481	2.0815763	0	0
COMPLEMENT	Hallmarks	105	0.5638298	2.0712934	0	0
INTERFERON_ALPHA_RESPONSE	Hallmarks	57	0.60117036	2.0018604	0	0
PROTEIN_SECRETION	Hallmarks	54	0.562084	1.8697265	0	0.001617046
COAGULATION	Hallmarks	77	0.5278026	1.8682957	0	0.001347538
TNF-A_SIGNALING_VIA_NFKB	Hallmarks	114	0.48063385	1.8070517	0	0.003266364
OXIDATIVE_PHOSPHORYLATION	Hallmarks	126	0.4268129	1.6279465	0	0.01873622
XENOBIOTIC_METABOLISM	Hallmarks	101	0.43746972	1.6219113	0	0.017550468
BILE_ACID_METABOLISM	Hallmarks	57	0.4702789	1.5808195	0.003378379	0.023945328
KRAS_SIGNALING_UP	Hallmarks	108	0.42079854	1.5409853	0.007861636	0.031320993
FATTY_ACID_METABOLISM	Hallmarks	81	0.39792186	1.4156573	0.025889968	0.0882699
UV_RESPONSE_UP	Hallmarks	82	0.39142403	1.4001218	0.032258064	0.09138525
P53_PATHWAY	Hallmarks	110	0.3703256	1.384519	0.0304414	0.09528734
E2F_TARGETS	Hallmarks	106	-0.45150977	-1.8036784	0	0.014216322
MYC_TARGETS_V1	Hallmarks	102	-0.42621982	-1.6953363	0	0.030741377
MYC_TARGETS_V2	Hallmarks	29	-0.5252515	-1.6048186	0.01627907	0.04516691
MITOTIC_SPINDLE	Hallmarks	110	-0.37685505	-1.5260106	0.007894737	0.06819525
NOTCH_SIGNALING	Hallmarks	20	-0.46811587	-1.3695186	0.101149425	0.19352844
G2M_CHECKPOINT	Hallmarks	108	-0.3323058	-1.341315	0.02610966	0.20183711

F

Type I IFN response genes

G

Type II IFN response genes

(legend on next page)

Immunoproteasome Deficiency Causes an Aberrant Proinflammatory Response in MT-MLs

We next investigated the cytokine and chemokine secretion profiles in PSC-MLs. IFN-α and IFN-β production was not observed in either WT-MLs or MT-MLs following IFN-γ and TNF-α or LPS stimulation (data not shown). IL-10 and IL-1β were also not detected in either WT-MLs or MT-MLs following IFN-γ and TNF-α stimulation (data not shown). However, IFN-γ and TNF-α stimulation significantly increased the secretion of proinflammatory cytokine IL-6 and proinflammatory chemokine MCP-1 in MT-MLs in comparison with the isogenic WT-ML counterparts (Figure 2A). Since an elevated IFN signature has been observed in other *PSMB8*-associated autoinflammatory diseases (Brehm et al., 2016; Liu et al., 2012), we next measured the secretion of an IFN-responsive chemokine, IP-10. The secretion of IP-10 in MT-MLs and WT-MLs did not differ to a statistically significant extent following IFN-γ and TNF-α stimulation (Figure 2B). However, upon stimulation with only type II (IFN-γ) or type I (IFN-α) IFN, MT-MLs secreted a significantly higher amount of IP-10 in comparison with WT-MLs (Figure 2C). Both type I and type II IFNs induced the robust secretion of IP-10. We therefore focused on the effect of type II IFN in the subsequent analysis. The increased production of IL-6 and IP-10 was confirmed with primary monocytes obtained from NNS patients (Figure S3E). Since the excessive secretion of these cytokine and chemokines from MT-MLs corresponds to previous serum cytokine levels in NNS patients (Arima et al., 2011), we considered our PSC-based *in vitro* model as having successfully recapitulated the cellular phenotypes of monocytic cells with an NNS-associated *PSMB8* mutation.

Untreated and Stimulated MT-MLs Show Distinct Proinflammatory Transcriptional Profiles

To reveal the specific inflammatory signatures of MT-MLs, we next performed RNA-sequencing (RNA-seq) analysis of the PSC-MLs. Most of the proteasome subunits, including β5i, β2i, and β1i, were upregulated upon IFN-γ and TNF-α treatment in both MT- and WT-MLs (Figure S3F). On the other hand, the expression of IFN-α or IFN-β genes was not detected even under the stimulated condition (Figure S3G). A principal component analysis from the normalized gene counts showed that the samples were clearly grouped according to the genotypes of *PSMB8* and stimulation (Figure 2D). MT-MLs and WT-MLs were distinguished even when untreated, indicating that *PSMB8*-mutant cells were in a "primed" state before stimulation. In order to extract differences in the regulation of the pathways in MT-MLs and WT-MLs, we performed a gene set enrichment analysis (Subramanian et al., 2005). Upon IFN-γ and TNF-α treatment of the MT-MLs, several inflammatory pathways, in particular interferon-associated pathways including "INTERFERON_GAMMA_RESPONSE," "INTERFERON_ALPHA_RESPONSE," and "TNF-A_SIGNALING_VIA_NF-κB," were significantly enriched (false discovery rate < 0.25; p < 0.01) in comparison with WT-MLs (Figure 2E). Especially, genes associated with type I and type II IFN responses were upregulated in MT-MLs (Figures 2F and 2G). These results suggest that the aberrant expression of genes, cytokines, and chemokines is associated with the *PSMB8* mutation even in an untreated state as well as in response to IFN-γ and TNF-α stimulation.

Since the NNS-associated *PSMB8* mutation is considered hypo-functional, we next wondered whether pharmacological inhibition of β5i could mimic the *in vitro* phenotypes of NNS. For this experiment, we pretreated PSC-MLs with a selective β5i inhibitor, ONX-0914 (Muchamuel et al., 2009), and evaluated the cytokine production. ONX-0914 decreased the chymotrypsin-like activity of WT-MLs stimulated with IFN-γ and TNF-α (Figure S4A). While a low dose of ONX-0914 increased the secretion of IL-6 and MCP-1, a high dose showed an anti-correlative inhibitory effect on the secretion of IL-6 and MCP-1, even though the chymotrypsin-like activity was inhibited (Figures S4B and S4C). On the other hand, the secretion of IP-10 from WT-MLs was reduced by pretreatment with ONX-0914 (Figures S4B and S4C). Since *PSMB8*-mutant MLs showed a consistent increase in the secretion of these cytokines, these results are inconsistent with

---

Figure 2. Functional Properties of PSC-MLs

(A and B) The amount of IL-6, MCP-1, and IP-10 secreted from PSC-MLs in response to treatment with IFN-γ (100 ng/mL) and TNF-α (100 ng/mL) for 20 hr. Bars indicate the means ±SD (*n* = 3). Asterisks indicate statistically significant differences by Student's t test: *p < 0.05; **p < 0.01.
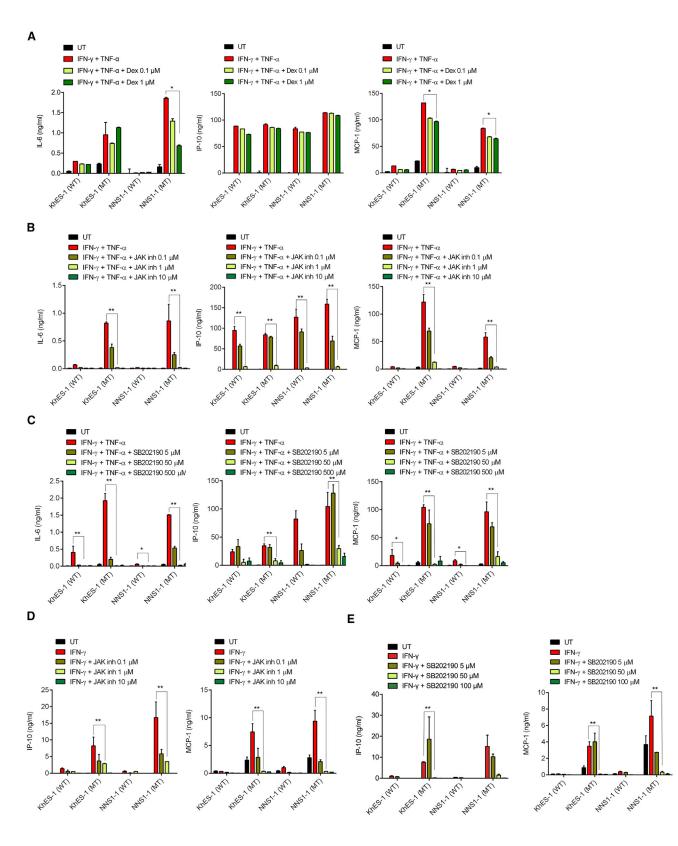
(C) The amount of IP-10 secreted in response to treatment with type II (IFN-γ, 100 ng/mL) or type I IFN (IFN-α) for 20 hr. Bars indicate the means ±SD (*n* = 3).

(D) A principal component analysis based on normalized RNA-seq data. Each symbol indicates each clone and treatment.

(E) Gene set enrichment analysis. Gene sets that were significantly (false discovery rate <0.25) enriched in MT-MLs treated with IFN-γ and TNF-α are shown.

(F and G) Heat maps of genes belonging to gene ontologies associated with type I (F) and type II (G) IFN responses. Columns are mean-centered with relative abundance represented by color (blue, lower abundance; red, higher abundance).

(legend on next page)

findings in NNS patients. The reason for this discrepancy is currently unknown, but we suppose it is associated with specific mutant *PSMB8* functions. Nevertheless, these data underscore the significance of mutant models instead of pharmacological models for the study of the NNS pathophysiology.

Effects of a Series of Anti-inflammatory Compounds on PSC-MLs Reveal the Specific Inflammatory Pathway in NNS

Because the cytokine assays and RNA-seq data indicated the activation of inflammatory pathways in MT-ML lines, we evaluated the effects of several anti-inflammatory compounds on IFN-γ- and TNF-α-treated PSC-MLs. First, PSC-MLs were pretreated with an anti-inflammatory corticosteroid, dexamethasone, which inhibits the activation of the NF-κB and MAPK pathways (Bhattacharyya et al., 2010). Dexamethasone slightly reduced the secretion of IL-6 and MCP-1, but not in all PSC-MLs, while the level of IP-10 was not affected (Figure 3A). Next, we attempted to inhibit downstream of the IFN pathway by using a pan-JAK inhibitor, tetracyclic pyridone 6 (P6) (Lucet et al., 2006; Pedranzini et al., 2006), a potent, cell-permeable, and ATP competitive inhibitor of JAK1, JAK2, JAK3, and Tyk2. P6 inhibited the secretion of IP-10, IL-6, and MCP-1 in a dose-dependent manner (Figure 3B). We also evaluated the effect of another JAK inhibitor, baricitinib, on IFN-γ- and TNF-α-treated PSC-MLs, because it is an approved drug and a clinical trial of baricitinib for CANDLE syndrome is ongoing (Jabbari et al., 2015). As expected, baricitinib inhibited the secretion of IP-10, IL-6, and MCP-1 in a dose-dependent manner (Figure S5).

Since the enhanced phosphorylation of p38 MAPK in inflamed tissue was observed in NNS patients (Arima et al., 2011), we wondered whether the enhanced p38 MAPK pathway was responsible for the proinflammatory response in MT-MLs. We therefore evaluated the effect of SB202190, a p38 MAPK inhibitor (Manthey et al., 1998). SB202190 inhibited the secretion of IL-6, IP-10, and MCP-1 in a dose-dependent manner (Figure 3C). Intriguingly, SB202190 and P6 showed similar potency at inhibiting the secretion of IP-10 and MCP-1 even under stimulation by IFN-γ alone (Figures 3D and 3E), indicating the possibility of pathological crosstalk between the IFN pathway and the p38 MAPK pathway in MT-MLs.

Excessive Production of Reactive Oxygen Species in MT-MLs Contributes to Proinflammatory Responses through Activation of the p38 MAPK and IFN-γ Pathways
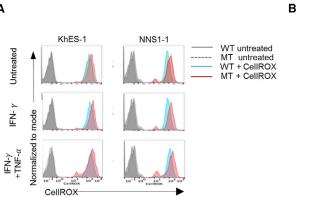
Impaired immunoproteasome activity can cause an abnormal accumulation of proteins and might therefore cause various stresses in cells. Proteasome dysfunction due to the use of the chemical inhibitor bortezomib causes damage to the mitochondria, leading the cells to increase their production of reactive oxygen species (ROS), which results in cytosolic oxidation (Maharjan et al., 2014). Oxidative stress can cause an increased production of inflammatory cytokines and chemokines (Naik and Dixit, 2011). Indeed, the intracellular production of ROS is increased in MT-MLs regardless of IFN-γ and TNF-α stimulation (Figures 4A and 4B). We therefore examined the effects of antioxidants on the production of cytokines and chemokines. The pretreatment of PSC-MLs with glutathione-SH (GSH) before IFN-γ and TNF-α stimulation reduced the secretion of IL-6 and MCP-1 (Figure 4C). In the presence of another antioxidant, N-acetyl-cysteine (NAC), the secretion of IL-6, MCP-1, and IP-10 was also significantly reduced (Figure 4D). Of note, higher concentrations of GSH or NAC markedly or completely inhibited the secretion of these cytokines and chemokines (Figures 4C and 4D). Interestingly, GSH and NAC also potently inhibited the secretion of IP-10 and MCP-1, even under stimulation with IFN-γ alone, indicating the contribution of ROS in the IFN-γ pathway in NNS (Figures 4E and 4F). Overall, these data indicate the important role that excessive ROS production plays in the proinflammatory response of NNS patient-derived monocytic cells. In previous reports, intracellular ROS was found to be an essential second messenger in various signal cascades (Yang et al., 2013). Proteasome dysfunction-mediated ROS can enhance the activation of the p38 MAPK pathway (Maharjan et al., 2014; Son et al., 2011), and the JAK/STAT pathway responds to intracellular ROS upon stimulation (Simon et al., 1998). Indeed, the phosphorylation of p38 MAPK in NNS patient lymphocytes was greater than that in healthy controls (Arima et al., 2011; Kitamura et al., 2011). Higher levels of phosphorylated STAT1 (pY701) and p38 MAPK (pT180/Y182) were observed in MT-MLs as well, even in an untreated state (Figure 5A), as too was the constitutive expression of p38 MAPK in MT-MLs (Figure 5A). The increased phosphorylation of STAT1 in untreated MT-MLs was ameliorated by NAC treatment
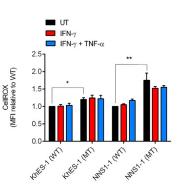

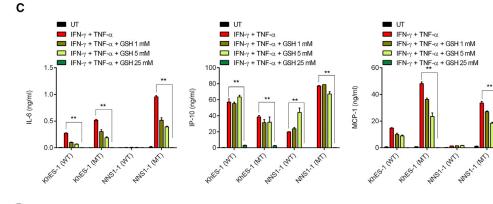**Figure 3. Effects of Anti-inflammatory Compounds on IFN-γ- and TNF-α-Treated PSC-MLs**

(A–E) The amount of IL-6, MCP-1, and IP-10 secreted from PSC-MLs. Cells were pretreated 3 hr with the indicated compounds and subsequently treated with IFN-γ and TNF-α (A–C) or IFN-γ only (D and E) for 20 hr. Bars indicate the means ±SD (n = 3). Asterisks indicate statistically significant differences by Student's t test: *p < 0.05; **p < 0.01.
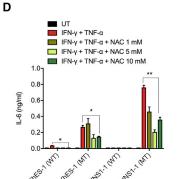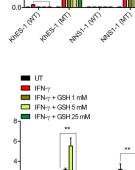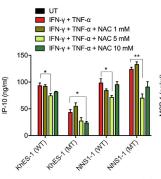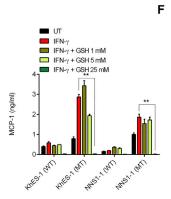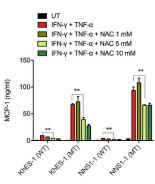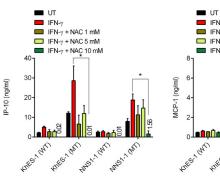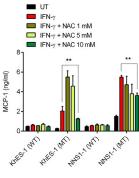
(legend on next page)

(Figure 5A). Interestingly, even in the stimulated condition, NAC treatment reduced the ratio of phospho-STAT1/total STAT1 in NNS patient-derived MT-MLs (Figure 5B). To elucidate the source of the ROS production, we next measured the production of mitochondrial ROS by using MitoSOX. Mitochondrial ROS was consistently increased in MT-MLs (Figures 5C and 5D). On the other hand, a NOX (NADPH oxidase) enzyme inhibitor, Apocynin, failed to inhibit ROS production or the secretion of IL-6, MCP-1, and IP-10 in all samples (Figures 5E–5G). Therefore, at least in our iPSC-based system, the primary source of ROS in MT-MLs seems to be mitochondria rather than NOX enzymes. This finding is consistent with a previous report that concluded the elevated ROS upon proteasomal inhibition originated from mitochondria (Maharjan et al., 2014).

Consequently, MT-MLs in the untreated state exhibited a "primed" state that coincides with excessive ROS production and with an inordinate amount of constitutively expressed STAT1. Engagement of the JAK/STAT and p38 MAPK pathways followed by IFN-γ and TNF-α stimulation in MT-MLs therefore elicited an augmented production of inflammatory cytokines and chemokines, part of which is mediated by the excessive production of ROS.

DISCUSSION

Recent advances in the field of proteasome diseases, including NNS, have revealed a critical connection between the dysregulation of the immunoproteasome and autoinflammation. However, the direct cause of the potent inflammation has not been fully elucidated. We herein established a panel of isogenic PSC clones by CRISPR/Cas9-mediated genome editing the *PSMB8* gene, which enabled us to precisely evaluate the *in vitro* phenotypes of PSC-derived differentiated progenies. We found that elevated ROS levels in MT-MLs have a pivotal role in the proinflammatory response and can be ameliorated by antioxidant therapy (Figure 6). Our PSC-based models therefore provide a possible alternative therapeutic option for NNS patients and may serve as a platform for seeking potential candidate compounds for medical use.

PRAASs are usually characterized by a type I IFN response. The primary source of type I IFN in CANDLE patients appears to be plasmacytoid dendritic cells (pDCs) (Brehm et al., 2015), but it is unknown whether the production of these cytokines is upregulated in the pDCs of NNS patients (Arima et al., 2011). Investigation should be given to whether pDCs from NNS-patient-derived iPSCs produce increased amounts of type I IFN, but currently there exists no reliable differentiation method from hPSCs toward pDCs. In the present study, we focused on the proinflammatory roles of monocytic cells in NNS rather than the production of type I or type II IFNs. We established the *in vitro* phenotypes of monocytic cells derived from PSCs and confirmed that these cells produce significant amounts of proinflammatory cytokines and chemokines under conditions that induce the immunoproteasome, suggesting a distinct role of these cells for maintaining the proinflammatory response in NNS.

Untreated MT-MLs showed lower chymotrypsin-like enzymatic activity than WT-MLs based on the constitutive expression of β5i (Figures 1E–1G). This observation is in line with previous findings that describe the constitutive expression of immunoproteasome components in hematopoietic cells, including monocytes, macrophages, B cells, and dendritic cells (Kimura et al., 2015; McCarthy and Weinberg, 2015). In our PSC-derived model, MT-MLs showed excessive production of ROS even in an untreated state, probably because of the constitutive accumulation of ubiquitinated proteins, which induced cellular stress (Figure 1H). Indeed, proteasome dysfunction is known to cause mitochondrial damage and subsequent mitochondrial and cellular ROS production (Maharjan et al., 2014). The excessive production of superoxide species then activates MAPK family molecules (Baas and Berk, 1995) and the JAK/STAT cascade (Simon et al., 1998), thereby causing a proinflammatory response by upregulating downstream inflammatory cytokines. Indeed, the enhanced phosphorylation of STAT1 was observed in untreated MT-MLs (Figure 5A), which is consistent with findings in NNS patient-derived fibroblasts, transformed B cells, and peripheral blood lymphocytes (Arima et al., 2011; Kitamura et al., 2011). Our data support the hypothesis that the excessive production of ROS is one of the direct downstream consequences of abnormal immunoproteasome function, connecting cellular stress to the activation of the proinflammatory pathway.
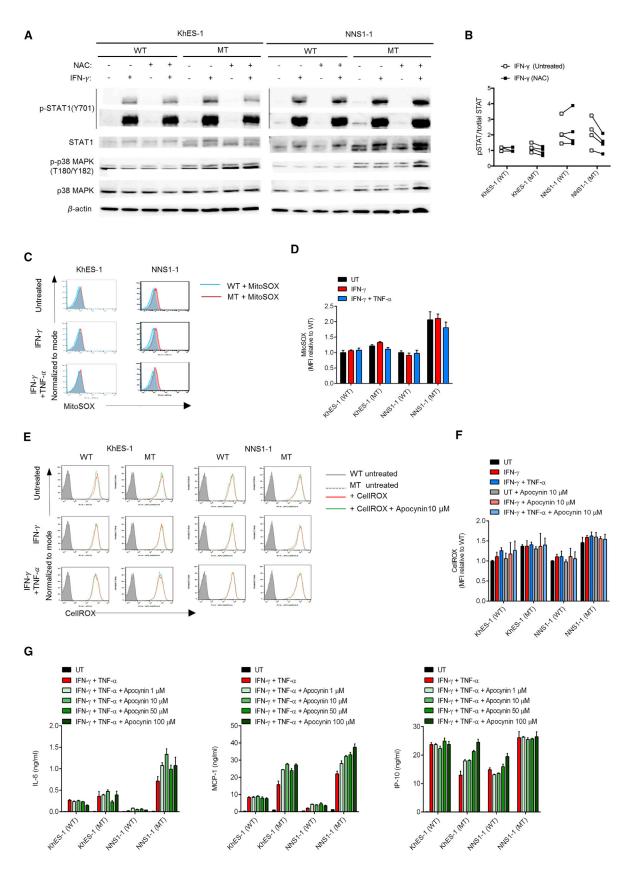
Figure 4. *PSMB8*-Mutant PSC-MLs Show Enhanced ROS Production
(A and B) ROS production in untreated PSC-MLs or those stimulated with IFN-γ with/without TNF-α measured by CellROX. Flow diagram (A) and quantification by mean fluorescence intensity (MFI) are shown (B).
(C and D) The amount of IL-6, MCP-1, and IP-10 secreted from PSC-MLs. Cells were pretreated for 3 hr with the indicated antioxidants and subsequently treated with IFN-γ and TNF-α for 20 hr.
(E and F) The amount of MCP-1 and IP-10 secreted from PSC-MLs. Cells were pretreated for 3 hr with the indicated antioxidants and subsequently treated with IFN-γ for 20 hr. IL-6 was not detected in this condition. Bars indicate the means ±SD (n = 3).
Asterisks indicate statistically significant differences by Student's t test: *p < 0.05; **p < 0.01.

(legend on next page)

In our model, ROS played a critical role in the excessive production of proinflammatory cytokines and chemokines, because antioxidative treatment inactivated the production of IL-6, MCP-1, and IP-10 through the p38 MAPK or JAK/STAT pathways. However, whether these pathways are necessary and sufficient for the pathogenesis of NNS remains to be elucidated, as proteasome dysregulation also causes other cellular stresses, such as endoplasmic reticulum stress (Otoda et al., 2013). Since antioxidant treatment did not reduce the accumulation of ubiquitinated proteins (Maharjan et al., 2014), a therapeutic approach that leads to the recovery of both cytokine overproduction and proteasome dysfunction could be required. Since the modulation of proteasome activity can be a promising therapeutic strategy for a variety of diseases (Huang and Chen, 2009) and the dysfunction of chymotrypsin-like proteasome activity is considered a primary cause of NNS (Kanazawa, 2012), we also tried to enhance chymotrypsin-like proteasome activity with betulinic acid (BA). The application of BA led to the recovery of the chymotrypsin-like activity in both MT- and WT-MLs in a dose-dependent manner (Figure S6A). However, the cytokine and chemokine production was not reduced in BA-treated PSC-MLs (Figure S6B), possibly due to BA off-target effects, such as activation of the p38 MAPK pathway (Tan et al., 2003). Consistent with a previous report (Trader et al., 2017), BA also failed to recover the constitutive accumulation of ubiquitinated proteins in MT-MLs (Figure S6C). These data indicate that, although it could upregulate chymotrypsin-like proteolytic activities, BA is insufficient for recovering the phenotypes associated with the disease-associated mutation. Therefore, further efforts are required to identify compounds that are effective at recovering immunoproteasome activities and resolving ubiquitinated proteins. We believe that our PSC-ML-based model can serve as a platform for high-throughput screening for finding these compounds, because this system enables functional assays to investigate the production of cytokines and the function of proteasomes in 96- or 384-well plates using immortalized PSC-MLs.

Interestingly, a JAK inhibitor, P6, suppressed the secretion of IL-6 and MCP-1, both of which are mainly depen-

dent on activation of the MAPK pathway (Figures 3B and 3D). On the other hand, a p38 MAPK inhibitor, SB202190, reduced not only the secretion of IL-6 and MCP-1, but also that of IP-10, which is mainly dependent on activation of the JAK/STAT pathway (Figures 3C and 3E). IFN-dependent production of IP-10 was suppressed by SB202190 even without TNF-α stimulation (Figure 3E). A part of this crosstalk seemed to occur under the influence of increased ROS, because an antioxidant, NAC, resolved the hyper-phosphorylation of STAT1 in unstimulated MT-MLs. Although the enhancement of STAT-dependent transcription by activation of the p38 MAPK pathway has been reported (Ramsauer et al., 2002), ROS-induced simultaneous activation of the p38 MAPK and JAK/STAT pathways has not. ROS may be a second messenger that enhances the p38 MAPK pathway, as NAC reduced the downstream cytokine production without affecting p38 MAPK phosphorylation (Figures 5A and 5B). Since the therapeutic use of p38 MAPK inhibitors or JAK inhibitors can be associated with severe side effects, such as secondary immune deficiency (Blume-Peytavi and Vogt, 2015; Sonbol et al., 2013), our results may support the possible use of antioxidants as an alternative therapeutic option for NNS and related immunoproteasome disorders (Figure 6).

Although progressive lipomuscular atrophy is an important phenotype that affects the quality of life of NNS patients, findings related to the functional roles of immunoproteasomes in affected tissues are relatively limited. Since PSCs can differentiate into other affected cells, such as myotubes and adipocytes, the tissue- or cell-type-specific pathophysiology of NNS can be explored using these progenies. The co-culturing of non-hematopoietic cells with PSC-derived immune cells will provide an opportunity for dissecting the cell-autonomous and non-cell-autonomous pathological mechanisms in muscle and adipose tissues. Our PSC-based methods can also be applicable to PRAAS. The validation of candidate compounds with these PSC-derived progenies is therefore an important step in the development of therapeutic applications for immunoproteasome diseases.

Figure 5. Enhanced Production of Mitochondrial ROS and Activation of the JAK/STAT Pathway in MT-MLs
(A) Western blotting analysis of whole-cell lysates of PSC-ML lines probed for total and phosphorylated STAT1 (pY701) or total and phosphorylated p38 MAPK (pT180/pY182). PSC-ML lines were pretreated with NAC for 3 hr and then with IFN-γ for 1 hr.
(B) Densitometric quantification of western blot bands of only the IFN-γ condition in (A). The NAC-treated group was measured by the fold change in the phosphorylation of STAT1/total STAT1 relative to the corresponding untreated group.
(C and D) Mitochondrial ROS production in PSC-MLs untreated or treated with IFN-γ with/without TNF-α measured by MitoSOX. Flow diagram (C) and quantification by mean fluorescence intensity (MFI) (D) are shown.
(E and F) ROS production in PSC-MLs untreated or treated with IFN-γ with/without TNF-α measured by CellROX in response to a NOX inhibitor, apocynin. Flow diagram (E) and quantification by MFI (F) are shown.
(G) The amount of IL-6, MCP-1, and IP-10 secreted from PSC-MLs. Cells were pretreated 3 hr with apocynin and subsequently treated with IFN-γ and TNF-α for 20 hr. (D, F, and G) Bars indicate the means ±SD (n = 3).
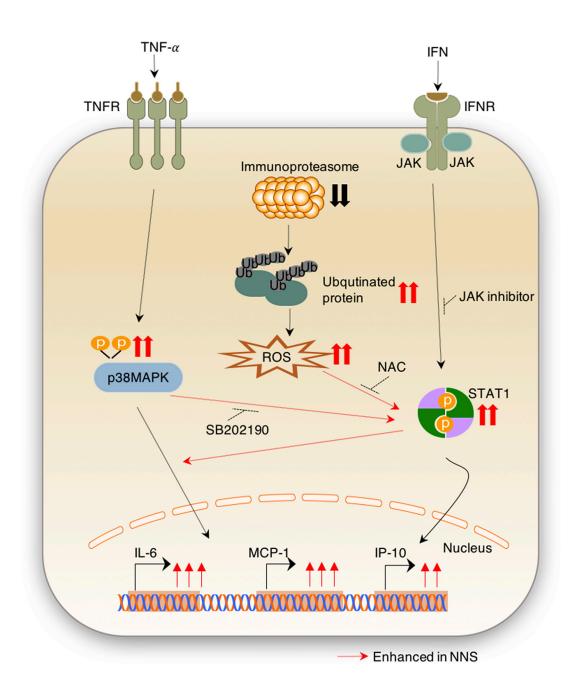
Figure 6. A Proposed Model of Autoinflammation Induced by *PSMB8* with the NNS-Associated Mutation

EXPERIMENTAL PROCEDURES

Please refer to the Supplemental Experimental Procedures for details of the methods.

Study Approval

This study was approved by the Ethics Committees of Kyoto University and Wakayama Medical University. Written informed consent was obtained from the patients or their guardians in accor-

dance with the Declaration of Helsinki. The use of human ESCs was approved by the Ministry of Education Culture, Sports, Science and Technology (MEXT) of Japan. The study plan for recombinant DNA research has been approved by the recombinant DNA experiments safety committee of Kyoto University.

Statistics

All statistical analyses were performed using Excel or R software programs. "n" stands for the number of independent experimental

replications. The values are presented as the mean ± SD. Statistical significance was evaluated using either Student's t test or the Wilcoxon rank-sum test.

ACCESSION NUMBERS

The accession number for the RNA-seq datasets reported in this paper is GEO: GSE111908.

SUPPLEMENTAL INFORMATION

Supplemental Information includes Supplemental Experimental Procedures, six figures, and three tables and can be found with this article online at https://doi.org/10.1016/j.stemcr.2018.04.004.

AUTHOR CONTRIBUTIONS

F.H-O. and M.T. performed almost all of the experiments. F.H-O., N.K., F.F., T.N., and M.K.S. designed the study. M.T., Y.K., H.I., and M.Y. performed the experiments. F.H-O., N.S., and A. Niwa analyzed the RNA-seq data. N.K. and F.F. recruited and evaluated the patients. A.H. and H.L.L. designed the genome-editing experiments. I.A., A. Nagahashi, and K.I. contributed to the establishment of iPSCs. F.H-O., A. Niwa, N.K., and M.K.S. wrote the manuscript. All of the authors read, edited, and approved the entire manuscript.

ACKNOWLEDGMENTS

REFERENCES

Almeida de Jesus, A., and Goldbach-Mansky, R. (2013). Monogenic autoinflammatory diseases: concept and clinical manifestations. Clin. Immunol. 147, 155–174.

Arima, K., Kinoshita, A., Mishima, H., Kanazawa, N., Kaneko, T., Mizushima, T., Ichinose, K., Nakamura, H., Tsujino, A., Kawakami, A., et al. (2011). Proteasome assembly defect due to a proteasome subunit beta type 8 (PSMB8) mutation causes the autoinflammatory disorder, Nakajo-Nishimura syndrome. Proc. Natl. Acad. Sci. USA 108, 14914–14919.

Atkinson, S.P., Collin, J., Irina, N., Anyfantis, G., Kyung, B.K., Lako, M., and Armstrong, L. (2012). A putative role for the immunoproteasome in the maintenance of pluripotency in human embryonic stem cells. Stem Cells 30, 1373–1384.

Baas, A.S., and Berk, B.C. (1995). Differential activation of mitogen-activated protein kinases by H2O2 and O2- in vascular smooth muscle cells. Circ. Res. 77, 29–36.

Bhattacharyya, S., Ratajczak, C.K., Vogt, S.K., Kelley, C., Colonna, M., Schreiber, R.D., and Muglia, L.J. (2010). TAK1 targeting by glucocorticoids determines JNK and IkappaB regulation in Toll-like receptor-stimulated macrophages. Blood 115, 1921–1931.

Blume-Peytavi, U., and Vogt, A. (2015). Translational positioning of Janus Kinase (JAK) inhibitors in alopecia areata. EBioMedicine 2, 282–283.

Brehm, A., Liu, Y., Sheikh, A., Marrero, B., Omoyinmi, E., Zhou, Q., Montealegre, G., Biancotto, A., Reinhardt, A., Almeida de Jesus, A., et al. (2015). Additive loss-of-function proteasome subunit mutations in CANDLE/PRAAS patients promote type I IFN production. J. Clin. Invest. 125, 4196–4211.

Brehm, A., Liu, Y., Sheikh, A., Marrero, B., Omoyinmi, E., Zhou, Q., Montealegre, G., Biancotto, A., Reinhardt, A., de Jesus, A.A., et al. (2016). Additive loss-of-function proteasome subunit mutations in CANDLE/PRAAS patients promote type I IFN production. J. Clin. Invest. 126, 795.

Ebstein, F., Kloetzel, P.M., Krüger, E., and Seifert, U. (2012). Emerging roles of immunoproteasomes beyond MHC class I antigen processing. Cell. Mol. Life Sci. 69, 2543–2558.

Garg, A., Hernandez, M.D., Sousa, A.B., Subramanyam, L., Martínez de Villarreal, L., dos Santos, H.G., and Barboza, O. (2010). An autosomal recessive syndrome of joint contractures, muscular atrophy, microcytic anemia, and panniculitis-associated lipodystrophy. J. Clin. Endocrinol. Metab. 95, E58–E63.

Groettrup, M., Kirk, C.J., and Basler, M. (2010). Proteasomes in immune cells: more than peptide producers? Nat. Rev. Immunol. 10, 73–78.

Haruta, M., Tomita, Y., Imamura, Y., Matsumura, K., Ikeda, T., Takamatsu, K., Nishimura, Y., and Senju, S. (2013). Generation of a large number of functional dendritic cells from human monocytes

expanded by forced expression of cMYC plus BMI1. Hum. Immunol. *74*, 1400–1408.

Huang, L., and Chen, C.H. (2009). Proteasome regulators: activators and inhibitors. Curr. Med. Chem. *16*, 931–939.

Jabbari, A., Dai, Z., Xing, L., Cerise, J.E., Ramot, Y., Berkun, Y., Sanchez, G.A., Goldbach-Mansky, R., Christiano, A.M., Clynes, R., et al. (2015). Reversal of alopecia areata following treatment with the JAK1/2 inhibitor Baricitinib. EBioMedicine *2*, 351–355.

Kanazawa, N. (2012). Nakajo-Nishimura syndrome: an autoinflammatory disorder showing pernio-like rashes and progressive partial lipodystrophy. Allergol. Int. *61*, 197–206.

Kawasaki, Y., Oda, H., Ito, J., Niwa, A., Tanaka, T., Hijikata, A., Seki, R., Nagahashi, A., Osawa, M., Asaka, I., et al. (2017). Identification of a high-frequency somatic NLRC4 mutation as a cause of autoinflammation by pluripotent cell-based phenotype dissection. Arthritis Rheumatol. *69*, 447–459.

Kimura, H., Caturegli, P., Takahashi, M., and Suzuki, K. (2015). New insights into the function of the immunoproteasome in immune and nonimmune cells. J. Immunol. Res. *2015*, 541984.

Kitamura, A., Maekawa, Y., Uehara, H., Izumi, K., Kawachi, I., Nishizawa, M., Toyoshima, Y., Takahashi, H., Standley, D.M., Tanaka, K., et al. (2011). A mutation in the immunoproteasome subunit *PSMB8* causes autoinflammation and lipodystrophy in humans. J. Clin. Invest. *121*, 4150–4160.

Kunimoto, K., Kimura, A., Uede, K., Okuda, M., Aoyagi, N., Furukawa, F., and Kanazawa, N. (2013). A new infant case of Nakajo-Nishimura syndrome with a genetic mutation in the immunoproteasome subunit: an overlapping entity with JMP and CANDLE syndrome related to *PSMB8* mutations. Dermatology *227*, 26–30.

Liu, Y., Ramot, Y., Torrelo, A., Paller, A.S., Si, N., Babay, S., Kim, P.W., Sheikh, A., Lee, C.C., Chen, Y., et al. (2012). Mutations in proteasome subunit β type 8 cause chronic atypical neutrophilic dermatosis with lipodystrophy and elevated temperature with evidence of genetic and phenotypic heterogeneity. Arthritis Rheum. *64*, 895–907.

Lucet, I.S., Fantino, E., Styles, M., Bamert, R., Patel, O., Broughton, S.E., Walter, M., Burns, C.J., Treutlein, H., Wilks, A.F., et al. (2006). The structural basis of Janus kinase 2 inhibition by a potent and specific pan-Janus kinase inhibitor. Blood *107*, 176–183.

Maharjan, S., Oku, M., Tsuda, M., Hoseki, J., and Sakai, Y. (2014). Mitochondrial impairment triggers cytosolic oxidative stress and cell death following proteasome inhibition. Sci. Rep. *4*, 5896.

Manthey, C.L., Wang, S.W., Kinney, S.D., and Yao, Z. (1998). SB202190, a selective inhibitor of p38 mitogen-activated protein kinase, is a powerful regulator of LPS-induced mRNAs in monocytes. J. Leukoc. Biol. *64*, 409–417.

McCarthy, M.K., and Weinberg, J.B. (2015). The immunoproteasome and viral infection: a complex regulator of inflammation. Front. Microbiol. *6*, 21.

McDermott, A., Jacks, J., Kessler, M., Emanuel, P.D., and Gao, L. (2015). Proteasome-associated autoinflammatory syndromes: advances in pathogeneses, clinical presentations, diagnosis, and management. Int. J. Dermatol. *54*, 121–129.

Muchamuel, T., Basler, M., Aujay, M.A., Suzuki, E., Kalim, K.W., Lauer, C., Sylvain, C., Ring, E.R., Shields, J., Jiang, J., et al. (2009). A selective inhibitor of the immunoproteasome subunit LMP7 blocks cytokine production and attenuates progression of experimental arthritis. Nat. Med. *15*, 781–787.

Murata, S., Yashiroda, H., and Tanaka, K. (2009). Molecular mechanisms of proteasome assembly. Nat. Rev. Mol. Cell Biol. *10*, 104–115.

Naik, E., and Dixit, V.M. (2011). Mitochondrial reactive oxygen species drive proinflammatory cytokine production. J. Exp. Med. *208*, 417–420.

Otoda, T., Takamura, T., Misu, H., Ota, T., Murata, S., Hayashi, H., Takayama, H., Kikuchi, A., Kanamori, T., Shima, K.R., et al. (2013). Proteasome dysfunction mediates obesity-induced endoplasmic reticulum stress and insulin resistance in the liver. Diabetes *62*, 811–824.

Pedranzini, L., Dechow, T., Berishaj, M., Comenzo, R., Zhou, P., Azare, J., Bornmann, W., and Bromberg, J. (2006). Pyridone 6, a pan-Janus-activated kinase inhibitor, induces growth inhibition of multiple myeloma cells. Cancer Res. *66*, 9714–9721.

Ramsauer, K., Sadzak, I., Porras, A., Pilz, A., Nebreda, A.R., Decker, T., and Kovarik, P. (2002). p38 MAPK enhances STAT1-dependent transcription independently of Ser-727 phosphorylation. Proc. Natl. Acad. Sci. USA *99*, 12859–12864.

Ran, F.A., Hsu, P.D., Lin, C.Y., Gootenberg, J.S., Konermann, S., Trevino, A.E., Scott, D.A., Inoue, A., Matoba, S., Zhang, Y., et al. (2013). Double nicking by RNA-guided CRISPR Cas9 for enhanced genome editing specificity. Cell *154*, 1380–1389.

Reis, J., Guan, X.Q., Kisselev, A.F., Papasian, C.J., Qureshi, A.A., Morrison, D.C., Van Way, C.W., 3rd, Vogel, S.N., and Qureshi, N. (2011). LPS-induced formation of immunoproteasomes: TNF-α and nitric oxide production are regulated by altered composition of proteasome-active sites. Cell Biochem. Biophys. *60*, 77–88.

Roccaro, A.M., Sacco, A., Aujay, M., Ngo, H.T., Azab, A.K., Azab, F., Quang, P., Maiso, P., Runnels, J., Anderson, K.C., et al. (2010). Selective inhibition of chymotrypsin-like activity of the immunoproteasome and constitutive proteasome in Waldenstrom macroglobulinemia. Blood *115*, 4051–4060.

Simon, A.R., Rai, U., Fanburg, B.L., and Cochran, B.H. (1998). Activation of the JAK-STAT pathway by reactive oxygen species. Am. J. Physiol. *275*, C1640–C1652.

Son, Y., Cheong, Y.K., Kim, N.H., Chung, H.T., Kang, D.G., and Pae, H.O. (2011). Mitogen-activated protein kinases and reactive oxygen species: how can ROS activate MAPK pathways? J. Signal Transduct. *2011*, 792639.

Sonbol, M.B., Firwana, B., Zarzour, A., Morad, M., Rana, V., and Tiu, R.V. (2013). Comprehensive review of JAK inhibitors in myeloproliferative neoplasms. Ther. Adv. Hematol. *4*, 15–35.

Subramanian, A., Tamayo, P., Mootha, V.K., Mukherjee, S., Ebert, B.L., Gillette, M.A., Paulovich, A., Pomeroy, S.L., Golub, T.R., Lander, E.S., et al. (2005). Gene set enrichment analysis: a knowledge-based approach for interpreting genome-wide expression profiles. Proc. Natl. Acad. Sci. USA *102*, 15545–15550.

Takahashi, K., Tanabe, K., Ohnuki, M., Narita, M., Ichisaka, T., Tomoda, K., and Yamanaka, S. (2007). Induction of pluripotent stem cells from adult human fibroblasts by defined factors. Cell *131*, 861–872.

Tan, Y., Yu, R., and Pezzuto, J.M. (2003). Betulinic acid-induced programmed cell death in human melanoma cells involves mitogen-activated protein kinase activation. Clin. Cancer Res. *9*, 2866–2875.

Trader, D.J., Simanski, S., Dickson, P., and Kodadek, T. (2017). Establishment of a suite of assays that support the discovery of proteasome stimulators. Biochim. Biophys. Acta *1861*, 892–899.

van Deventer, S., and Neefjes, J. (2010). The immunoproteasome cleans up after inflammation. Cell *142*, 517–518.

Yanagimachi, M.D., Niwa, A., Tanaka, T., Honda-Ozaki, F., Nishimoto, S., Murata, Y., Yasumi, T., Ito, J., Tomida, S., Oshima, K., et al. (2013). Robust and highly-efficient differentiation of functional monocytic cells from human pluripotent stem cells under serum- and feeder cell-free conditions. PLoS One *8*, e59243.

Yang, C.S., Kim, J.J., Lee, S.J., Hwang, J.H., Lee, C.H., Lee, M.S., and Jo, E.K. (2013). TLR3-triggered reactive oxygen species contribute to inflammatory responses by activating signal transducer and activator of transcription-1. J. Immunol. *190*, 6368–6377.

Yun, Y.S., Kim, K.H., Tschida, B., Sachs, Z., Noble-Orcutt, K.E., Moriarity, B.S., Ai, T., Ding, R., Williams, J., Chen, L., et al. (2016). mTORC1 coordinates protein synthesis and immunoproteasome formation via PRAS40 to prevent accumulation of protein stress. Mol. Cell *61*, 625–639.

Zhou, J., Wang, J., Shen, B., Chen, L., Su, Y., Yang, J., Zhang, W., Tian, X., and Huang, X. (2014). Dual sgRNAs facilitate CRISPR/Cas9-mediated mouse genome targeting. FEBS J. *281*, 1717–1725.